ISSN 1070-4280, Russian Journal of Organic Chemistry, 2020, Vol. 56, No. 11, pp. 1982–1994. © Pleiades Publishing, Ltd., 2020.

Synthesis, Spectroscopic and Computational Analysis of 2-[(2-Sulfanyl-1*H*-benzo[*d*]imidazol-5-yl)iminomethyl]-phenyl Naphthalene-2-sulfonate

G. Kotan[a],*, H. Gökce[b], O. Akyıldırım[c], H. Yüksek[d], M. Beytur[d], S. Manap[d], and H. Medetalibeyoğlu[d]

[a] *Kars Vocational School, Kafkas University, Kars, 36100 Turkey*
[b] *Vocational School of Health Services, Giresun University, Giresun, 28200 Turkey*
[c] *Department of Chemical Engineering, Faculty of Engineering and Architecture, Kafkas University, Kars, 36100 Turkey*
[d] *Department of Chemistry, Kafkas University, Kars, 36100 Turkey*
**e-mail: gulkemer@hotmail.com*

Received April 20, 2019; revised May 1, 2020; accepted May 9, 2020

Abstract—2-[(2-Sulfanyl-1*H*-benzo[*d*]imidazol-5-yl)iminomethyl]phenyl naphthalene-2-sulfonate was obtained as a result of the reactions of 5-amino-2-sulfanylbenzimidazole with 2-(2-naphthylsulfonyloxy)benzaldehyde. The newly synthesized compound was characterized using IR, ^{1}H and ^{13}C NMR spectroscopy. Theoretical investigations of the thione–thiol tautomerism of the molecule were performed using DFT/ B3LYP calculations with the 6-311++G(d,p) basis set. The NMR chemical shifts were calculated by the gauge-invariant atomic orbital (GIAO) method and compared with the experimental data. Additionally, the frontier molecular orbital (HOMO-LUMO), MEP, and NLO analyses were performed for the optimized structure. The NLO analysis showed that the thiol form of the molecule is more stable than the thione form and is a good non-linear optical compound.

Keywords: imines derivative, GIAO, MEP, HOMO, LUMO, NLO

DOI: 10.1134/S1070428020110135

INTRODUCTION

Benzimidazoles occupy special place among biologically active heterocyclic compounds. Benzimidazole derivatives comprising a Schiff base moiety have shown diverse biological activities, including antioxidant [1–3], analgesic [4–6], anti-inflammatory [7–9], antidiabetic [10], antimicrobial [11–13], antitumor [14–16], antihistamines [17, 18], antihypertensive [19–21], antiviral [22–24], and antifungal [25–27]. Sulfur-containing benzimidazole derivatives, specifically 2-sulfanylbenzimidazoles (**2-SBI**), have exhibited anticonvulsant properties [28]. Therefore, organic chemists synthesized a variety of functionally substituted 2-sulfanylbenzimidazoles [29].

Thus, we report the synthesis of a novel 2{(2-sulfanyl-1*H*-benzo[*d*]imidazol-5-yl)iminomethyl}phenyl naphthalene-2-sulfonate (**2-SBNS**) and its quantum chemical computations. To the best of our knowledge, the synthesis and quantum-chemical investigation of the **2-SBNS** compound was not reported.

RESULTS AND DISCUSSION

2-{(2-Sulfanyl-1*H*-benzo[*d*]imidazol-5-yl)iminomethyl}phenyl naphthalene-2-sulfonate (**2-SBNS**) was synthesized as shown in Scheme 1. The first stage involved the synthesis of 2-[(naphthalene-2-yl)sulfonyloxy]benzaldehyde (**1**) by the reaction of 2-hydroxybenzaldehyde with naphthalene-2-sulfonyl chloride. At the second stage, compound **1** was reacted with 5-amino-2-sulfanylbenzimidazole (**2**) in acetic acid to obtain the target **2-SBNS**.

The structure of the synthesized compound suggested its existence in the thiol and thione forms (Scheme 2). Therefore, the theoretical investigation of **2-SBNS** was focused on the features of the thiol–thione tautomerism of this compound.

Scheme 1.

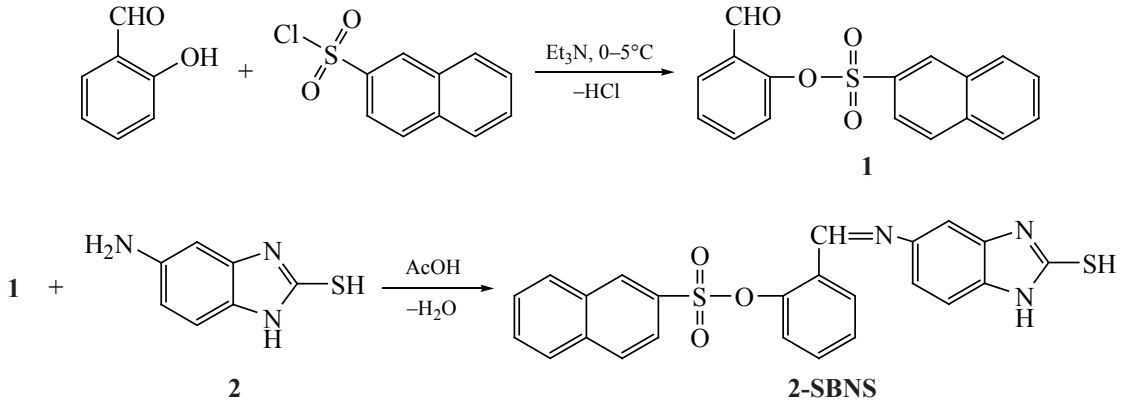

Molecular Geometry. The molecular geometry features, such as the Mulliken atomic charges, bond angles and bond lengths for the thiol and thione forms of the optimized molecule (Fig. 1) were calculated using the B3LYP functional in the DFT method with the 6-311++G(d,p) basis set [30–32] (Tables 1 and 2). The longest in **2-SBNS** is the S^{49}–C^{15} bond (1.783/1.782 Å for the thiol and thione forms, respectively). Besides, significant lengths are found for the N^{42}–C^{1}, N^{43}–C^{1}, C^{3}–N^{42}, C^{2}–C^{3}, C^{7}–N^{44}, and C^{8}–N^{44}: 1.377/1.378, 1.374/1.374, 1.389/1.390, 1.410/1.403, 1.397/1.399, and 1.276/1.280 Å, respectively (Table 1). The largest bond angle is N^{42}–C^{3}–C^{4} (132.295/132.935°) for the thiol and thione forms, respectively (Table 1). The theoretical calculations relate to the gas phase. As seen, the calculated bond angles and lengths for the thiol and thione forms have different values.

Scheme 2.

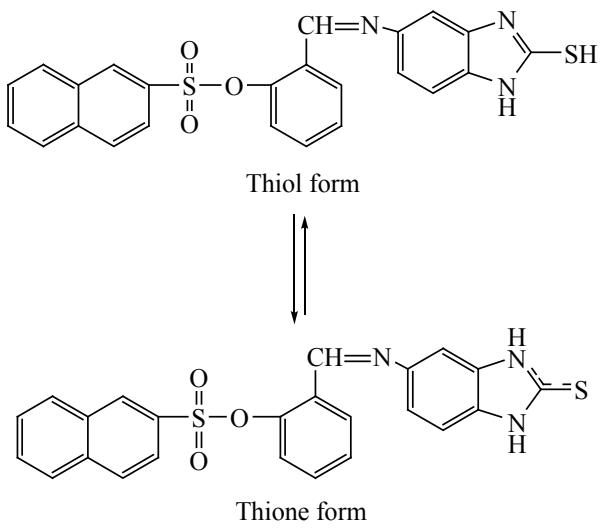

The Mulliken atomic charge distributions were also obtained. The electronegative N, S, and O atoms have negative charges. The highest positive charges are on C^{9} in both forms: 1.187 (thiol) and 1.124 (thione). All hydrogen atoms (H^{25}–H^{41}) have positive atomic charge values (Table 2).

^{1}H and ^{13}C NMR chemical shifts. The experimental and theoretical ^{1}H and ^{13}C NMR chemical shifts for **2-SBNS**, calculated by the gauge invariant atomic orbitals (GIAO) method [33] are listed and compared in Table 3. In the experimental ^{1}H NMR spectrum of **2-SBNS**, the signal of the benzimidazole ring NH proton appears at 12.56 ppm and the signal of the SH proton, at 12.29 ppm. The calculated ^{1}H NMR chemical shifts of the benzimidazole ring NH proton signal are 9.78 (vacuum) and 9.63 (DMSO) ppm, and the calculated ^{1}H NMR chemical shifts of the SH proton signal are 9.58 (vacuum) and 9.70 (DMSO) ppm. The aromatic CH protons gives broad peaks at 6.73–8.11 ppm in the experimental ^{1}H NMR spectrum, and the calculated chemical shifts for the signals of these protons are 7.46–8.92 (vacuum) and 7.91–9.22 (DMSO) ppm.

The calculated ^{13}C NMR chemical shifts range from ~ 170.0 to < 100.0 ppm (Table 3). The experimental chemical shift of the C^{1}=S^{28} carbon is 145.68 ppm. The chemical shift values of C^{1} atom bounded sulfur atom (C^{1}=S^{28}) have been calculated at 150.32 (vacuum) and 154.20 (DMSO) ppm, respectively. The calculated ^{13}C NMR chemical shifts of aromatic C atoms range from ~ 160.0 to < 110.0 ppm (both vacuum and DMSO). The calculated values for the imino C^{8}=N carbon atom are 159.37 (vacuum) and 160.73 (DMSO) ppm, while the esperimental value for this carbon atom 168.88 ppm. As seen from Table 3, the calculated ^{13}C NMR chemical

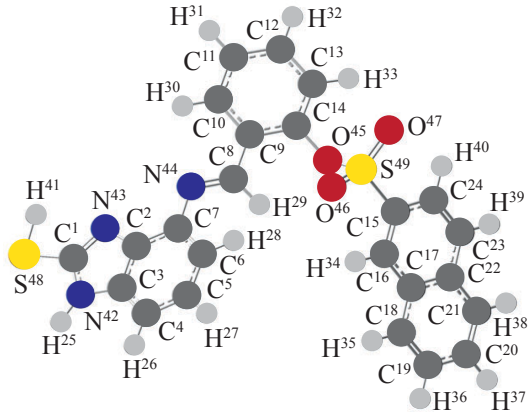

Fig. 1. Optimized structure of **2-SBNS** with atom numbering.

shifts of **2-SBNS** are generally closer than ^{1}H NMR chemical shifts to experimental.

The following correlation equations were obtained for the experimental and calculated ^{13}C NMR chemical shifts: R^2 correlation coefficients are as follows: $\delta(exp) = 1.0088\delta(calc) - 17.227$, ($R^2 = 0.9231$) in vacuum, $\delta(exp) = 1.1035\delta(calc) - 19.777$, ($R^2 = 0.9254$) in DMSO. The respecive correlation coefficients for the ^{1}H NMR chemical shifts are as follows: $\delta(exp) = 2.1331\delta(calc) - 9.8805$, ($R^2 = 0.5639$) in vacuum, $\delta(exp) = 1.8283\delta(calc) - 7.1391$, ($R^2 = 0.6238$) in DMSO. The fact that the correlations for the ^{1}H NMR chemical shifts are much poorer than for the ^{13}C NMR chemical shifts ($R^2 = 0.9231$ and 0.9254 versus 0.5639 and 0.6238, respectively) can be explained by the acidity of the benzimidazole NH and SH groups.

IR spectral analysis. Based on the optimized geometries, we calculated the vibrational frequencies by the Veda4 program [34]. The calculated harmonic vibrational frequencies were multiplied by the scale factor 0.9688 [35]. Table 4 compares the experimental and calculated values. The bands calculated in the measured region 4000–400 cm^{-1} arise from the N–H and S–H stretching, methyl asymmetric and symmetric stretching vibrations of **2-SBNS**. The vibration bands were assigned using the GaussView molecular visualization program (Fig. 2) [36]. The theoretical and experimental vibrational frequencies of **2-SBNS** are listed in Table 4. Most bands observed in the IR spectra belong to both forms. The calculated frequencies for these bands are 3067, 1557, 1369 cm^{-1} for the thiol form and 2987, 1559, 1376 cm^{-1} for the thione form. The vibration bands of the aromatic ring in the experimental IR spectrum are observed at 2961, 1549 and 1373 cm^{-1}. The calculated values for the thione and thiol forms are 2987 and 3067 cm^{-1}, respectively. The benzimidazole S–H and C=N stretching modes are observed at 2863 and 1610 cm^{-1} (experiment), and the respective calculated values are 3006 and 1611 cm^{-1} (thiol) and

Table 1. Calculated bond lengths (Å) and bond angles (deg) for the thiol and thione forms of **2-SBNS**

Bond angles	Thiol form	Thione form	Bond angles	Thiol form	Thione form	Bond lengths	Thiol form	Thione form
N^{42}–C^{1}–N^{43}	113.586	104.536	O^{45}–S^{19}–C^{15}	96.980	97.040	C^{1}–N^{42}	1.377	1.378
N^{42}–C^{1}–S^{48}	120.368	127.495	O^{46}–S^{49}–C^{15}	110.104	110.111	C^{1}–N^{43}	1.374	1.374
C^{1}–S^{48}–H^{41}	93.110	–	O^{47}–S^{49}–C^{15}	110.084	110.344	C^{1}–S^{48}	1.766	1.664
C^{1}–N^{43}–C^{2}	104.874	111.417	S^{49}–C^{15}–C^{16}	118.690	118.735	S^{48}–H^{41}	1.346	–
N^{42}–C^{3}–C^{2}	104.434	105.701	S^{49}–C^{15}–C^{24}	118.916	118.840	N^{42}–H^{25}	1.007	1.007
N^{42}–C^{3}–C^{4}	132.295	132.935	C^{15}–C^{16}–H^{34}	120.337	120.362	N^{42}–C^{3}	1.389	1.390
C^{3}–C^{4}–C^{5}	116.258	116.899	C^{15}–C^{16}–C^{17}	119.520	119.506	C^{2}–C^{3}	1.410	1.403
H^{25}–N^{42}–C^{3}	126.764	–	H^{34}–C^{16}–C^{17}	120.140	120.130	C^{3}–C^{4}	1.392	1.389
C^{3}–C^{4}–H^{26}	122.248	121.757	C^{16}–C^{17}–C^{18}	121.771	121.772	C^{4}–H^{26}	1.083	1.082
H^{26}–C^{4}–C^{5}	121.490	121.337	C^{16}–C^{17}–C^{22}	119.007	118.993	C^{4}–C^{5}	1.392	1.398
C^{4}–C^{5}–C^{6}	121.777	121.971	C^{17}–C^{22}–C^{23}	119.112	119.130	C^{5}–H^{27}	1.084	1.083
C^{4}–C^{5}–H^{27}	119.291	119.039	C^{22}–C^{23}–H^{39}	118.906	118.904	C^{5}–C^{6}	1.402	1.396
H^{27}–C^{5}–C^{6}	118.928	118.982	H^{39}–C^{23}–C^{24}	119.897	119.888	C^{6}–H^{28}	1.083	1.083

Table 1. (Contd.)

Bond angles	Thiol form	Thione form	Bond angles	Thiol form	Thione form	Bond lengths	Thiol form	Thione form
$C^5–C^6–H^{28}$	119.435	119.514	$C^{23}–C^{24}–H^{40}$	121.371	121.332	$C^6–C^7$	1.402	1.407
$C^5–C^6–C^7$	121.873	121.971	$H^{40}–C^{24}–C^{15}$	119.853	119.926	$C^7–N^{44}$	1.397	1.399
$H^{28}–C^6–C^7$	118.634	118.982	$C^{17}–C^{18}–H^{35}$	118.895	118.918	$C^8–N^{44}$	1.276	1.280
$C^6–C^7–C^2$	117.019	116.217	$C^{17}–C^{18}–C^{19}$	120.550	120.539	$C^8–H^{29}$	1.092	1.090
$C^2–C^3–C^4$	123.271	121.362	$H^{35}–C^{18}–C^{19}$	120.556	120.543	$C^8–C^9$	1.469	1.465
$C^7–N^{42}–C^8$	119.802	119.924	$C^{18}–C^{19}–C^{20}$	120.290	120.285	$C^9–C^{10}$	1.404	1.404
$N^{44}–C^8–H^{29}$	121.874	121.790	$C^{19}–C^{20}–C^{21}$	120.523	120.536	$C^{10}–H^{30}$	1.083	1.404
$N^{44}–C^8–C^9$	121.492	121.861	$C^{20}–C^{21}–C^{22}$	120.687	120.679	$C^{10}–C^{11}$	1.387	1.386
$C^8–C^9–C^{10}$	121.064	121.414	$C^{17}–C^{22}–C^{21}$	118.730	118.726	$C^{11}–H^{31}$	1.083	1.082
$C^8–C^9–C^{14}$	121.329	120.987	$H^{36}–C^{19}–C^{20}$	119.598	119.601	$C^{11}–C^{12}$	1.397	1.386
$C^9–C^{10}–C^{11}$	121.005	121.068	$C^{19}–C^{20}–H^{37}$	119.501	119.493	$C^{12}–H^{32}$	1.083	1.083
$C^9–C^{10}–H^{30}$	117.664	117.903	$H^{37}–C^{20}–C^{21}$	119.976	119.972	$C^{12}–C^{13}$	1.390	1.397
$H^{30}–C^{10}–C^{11}$	121.331	121.028	$C^{20}–C^{21}–H^{38}$	120.416	120.403	$C^{13}–H^{33}$	1.081	1.083
$C^{10}–C^{11}–H^{31}$	119.854	119.892	$H^{38}–C^{21}–C^{22}$	118.897	119.972	$C^{13}–C^{14}$	1.391	1.390
$C^{10}–C^{11}–C^{12}$	120.153	120.090				$C^{14}–O^{45}$	1.404	1.401
$C^{11}–C^{12}–C^{13}$	120.053	120.089				$O^{45}–S^{49}$	1.680	1.684
$H^{31}–C^{11}–C^{12}$	119.993	120.018				$O^{46}–S^{49}$	1.455	1.456
$C^{11}–C^{12}–H^{32}$	120.310	120.271				$S^{49}–O^{47}$	1.454	1.454
$H^{32}–C^{12}–C^{13}$	119.636	119.640				$S^{49}–C^{15}$	1.783	1.782
$C^{12}–C^{13}–H^{33}$	121.513	121.453				$C^{15}–C^{16}$	1.372	1.372
$C^{12}–C^{13}–C^{14}$	119.209	119.297				$C^{16}–H^{34}$	1.083	1.083
$H^{33}–C^{13}–C^{14}$	119.276	119.250				$C^{16}–C^{17}$	1.417	1.417
$C^{14}–O^{45}–S^{49}$	118.526	118.893				$C^{17}–C^{18}$	1.419	1.419
$O^{45}–S^{49}–O^{46}$	108.150	107.806				$C^{17}–C^{22}$	1.431	1.431
$O^{45}–S^{49}–O^{47}$	108.285	108.188				$C^{22}–C^{23}$	1.421	1.418
$O^{46}–S^{49}–O^{47}$	120.597	120.682				$C^{23}–H^{39}$	1.084	1.084
						$C^{23}–C^{24}$	1.371	1.421
						$C^{24}–H^{40}$	1.082	1.084
						$C^{18}–H^{35}$	1.084	1.082
						$C^{18}–C^{19}$	1.373	1.373
						$C^{19}–H^{36}$	1.083	1.083
						$C^{19}–C^{20}$	1.414	1.414
						$C^{20}–H^{37}$	1.084	1.084
						$C^{20}–C^{21}$	1.374	1.374
						$C^{21}–H^{38}$	1.084	1.084
						$C^{21}–C^{22}$	1.418	1.418

Table 2. Calculated Mulliken atomic charges for **2-SBNS**

Atom	Thiol form, DFT	Thione form, DFT	Atom	Thiol form, DFT	Thione form, DFT
C^{1}	0.462	0.336	H^{25}	0.174	0.178
C^{2}	0.017	–0.034	H^{26}	0.186	0.100
C^{3}	0.282	0.214	H^{27}	0.135	0.138
C^{4}	–0.423	–0.340	H^{28}	0.217	0.193
C^{5}	0.381	–0.320	H^{29}	0.175	0.185
C^{6}	–0.194	–0.174	H^{30}	0.179	0.181
C^{7}	–0.007	0.265	H^{31}	0.195	0.188
C^{8}	–0.431	–0.364	H^{32}	0.169	0.164
C^{9}	1.187	1.124	H^{33}	0.134	0.138
C^{10}	–0.532	–0.158	H^{34}	0.178	0.178
C^{11}	–0.549	–0.015	H^{35}	0.175	0.177
C^{12}	–0.254	–0.229	H^{36}	0.132	0.133
C^{13}	–0.075	–0.578	H^{37}	0.154	0.157
C^{14}	–0.039	–0.520	H^{38}	0.215	0.215
C^{15}	–0.451	–0.402	H^{39}	0.097	0.337
C^{16}	–0.121	–0.116	N^{42}	–0.188	–0.194
C^{17}	0.140	–0.116	N^{43}	–0.047	–0.162
C^{18}	–0.168	0.169	N^{44}	0.252	0.153
C^{19}	–0.301	–0.290	O^{45}	0.104	0.096
C^{20}	–0.167	–0.171	O^{46}	–0.013	–0.014
C^{21}	–0.136	–0.137	O^{47}	–0.009	–0.015
C^{22}	0.328	0.305	S^{48}	–0.489	–0.525
C^{23}	0.239	–0.222	S^{49}	–0.574	–0.712
C^{24}	0.032	0.018			

2610 and 1611 cm^{-1} (thione). Two weak bands at 1275 and 1043 cm^{-1} in the experimental spectrum were assigned to S=O and S–O vibrations. The calculated R^2 results of **2-SBNS** have been 0.9991 for thiol and 0.9921 for thione form. R^2 correlation coefficients are as follows: $\delta(exp) = 0.9400\delta(calc) + 51.433$, ($R^2 = 0.9991$) for thiol, $\delta(exp) = 0.9853\delta(calc) + 20.555$ ($R^2 = 0.9921$) for thione. The experimental and calculated harmonic vibrational frequencies of **2-SBNS** were found a linear correlation.

HOMO-LUMO analysis. Frontier molecular orbitals (HOMO and LUMO) relate to kinetic stability, electronic transitions, and electric and optical properties [37]. The energy difference between the LUMO and HOMO is termed the HOMO-LUMO gap (ΔEg). The ΔEg values of **2-SBNS** calculated by using the B3LYP functional in the DFT method with the 6-311++G(d,p) basis set for the thiol and thione forms are 3.5918 and 3.167 eV, respectively (Fig. 3). The figure shows the HOMO and LUMO surfaces for **2-SBNS**. As seen, in the LUMO, electrons are mainly delocalized on the sulfonyloxy group and the naphthalene ring, whereas in the HOMO, along with the sulfonyloxy group and the naphthalene ring, electrons are also delocalized on the

Table 3. Experimental (DMSO-d_6) and calculated ^{1}H and ^{13}C NMR isotropic chemical shifts (δ, ppm) for **2-SBNS**

Atom	Exp.[a]	Calc.[a] (vacuum)	Exp.-Calc. (vacuum)	Calc. (DMSO)	Exp.-Calc. (DMSO)	Atom	Exp.	Calc. (vacuum)	Exp.-Calc. (vacuum)	Calc. (DMSO)	Exp.-Calc. (DMSO)
C^1	145.68	150.32	–4.64	154.2	–8.52	H^{25}	12.56	9.78	2.78	9.63	2.93
C^2	135.12	145.13	–10.01	144.12	–9.00	H^{26}	6.73	7.76	–1.03	7.42	–0.69
C^3	132.63	141.73	–9.10	142.64	–10.01	H^{27}	6.77	8.02	–1.25	7.52	–0.75
C^4	101.60	108.29	–6.69	111.36	–9.76	H^{28}	7.03	8.03	–1.00	7.34	–0.31
C^5	122.19	127.44	–5.25	128	–5.81	H^{29}	8.57	8.81	–0.24	9.22	–0.65
C^6	109.86	114.76	–4.90	114.47	–4.61	H^{30}	8.11	8.72	–0.61	8.94	–0.83
C^7	148.85	151.87	–3.02	149.88	–1.03	H^{31}	7.47	8.30	–0.83	7.83	–0.36
C^8	168.88	159.37	9.51	160.73	8.15	H^{32}	7.57	8.33	–0.76	7.93	–0.36
C^9	131.24	138.55	–7.31	137.5	–6.26	H^{33}	7.25	7.46	–0.21	7.91	–0.66
C^{10}	152.33	156.42	–4.09	156.27	–3.94	H^{34}	8.32	8.61	–0.29	9.01	–0.69
C^{11}	127.64	130.17	–2.53	133.04	–5.40	H^{35}	8.05	8.95	–0.90	8.43	–0.38
C^{12}	130.26	135.99	–5.73	138.3	–8.04	H^{36}	7.62	7.47	0.15	7.98	–0.36
C^{13}	127.83	131.71	–3.88	130.80	–2.97	H^{37}	7.71	8.51	–0.80	8.05	–0.34
C^{14}	128.07	134.13	–6.06	132.90	–4.83	H^{38}	7.80	8.78	–0.98	8.31	–0.51
C^{15}	132.85	143.98	–11.13	142.43	–9.58	H^{39}	7.96	8.85	–0.89	8.44	–0.48
C^{16}	129.05	134.74	–5.69	135.11	–6.06	H^{40}	8.11	8.92	–0.81	9.22	–1.11
C^{17}	130.82	136.69	–5.87	136.39	–5.57	H^{41}	12.59	9.58	3.01	9.70	2.89
C^{18}	130.11	135.39	–5.28	135.79	–5.68						
C^{19}	127.90	132.12	–4.22	133.44	–5.54						
C^{20}	129.51	134.98	–5.47	136.69	–7.18						
C^{21}	127.64	131.66	–4.02	132.26	–4.62						
C^{22}	131.43	139.84	–8.41	140.15	–8.72						
C^{23}	127.94	133.50	–5.56	135.07	–7.13						
C^{24}	123.61	127.40	–3.79	125.86	–2.25						

[a] Here and hereinafter: (Exp.) experimental and (Calc.) calculated values.

benzimidazole ring. The thione form is lower in energy compared to the thiol form, and, therefore, is more stable. By using LUMO-HOMO, we also calculated the softness (*S*), ionization potential (*I*), electronegativity (χ), chemical potential (P_i), global hardness (η), electron affinity (*A*), nucleophilic index (*IP*), chemical potential (μ) and electrophilic index (ω) for **2-SBNS** (Table 5).

Thermodynamics properties. Thermodynamic parameters were calculated by the DFT/B3LYP/6-311G++(d,p) method for a pressure of 1 atm and a temperature of 298.150 K. The calculated translational, rotational, vibrational, entropy and enthalpy parameters. The calculated thermal energy (*E*), entropy (*S*) and heat capacity (C_V) are 242.073/244.433 kcal/mol; 188.256/185.356; 104.630/103.612 cal mol^{-1} K for the thione and thiol forms, respectively (Table 6).

The calculated zero-point vibration energies (ZPVE) were 225.245717 and 227.98331 kcal/mol for the thiol and thione forms, respectively.

Table 4. Principal experimental and calculated IR frequencies for **2-SBNS** (cm^{-1})

Vibrational modes (PED, %)[a]	Exp.	Thiol form (scaled B3LYP)	Thione form (scaled B3LYP)
τ CCCC(14), ν CC(39)	623	620	621
τ SNNC(30), τ CNCN(29)	659	648	657
τ CCCC(12), τ CNCN(12), τ CCCN(11)	775	762	767
τ CCCC(18), τ CNCC(13)	814	817	815
δ CCC(11), τ HCNC(13)	847	848	843
τ CNNC(29)	870	869	869
τ HCCC(32)	973	976	970
ν SO(23), ν CC(18), δ HCC(15)	1043	1050	1044
ν OC(10), δ CCC(14)	1079	1075	1074
ν CC(11), ν OC(17), δ HCC(23)	1163	1184	1152
ν SO(85)	1275	1289	1273
ν CC (13), ν NC(17), δ HNC(21)	1373	1369	1376
ν CC(28), δ HCC(11)	1549	1557	1559
ν NC(29), δ HCC(15)	1610	1611	1611
ν SH(100)	2863	3006	2610
ν CH(59)	2961	3067	2987
ν NH(100)	3333	3551	3544

[a] Vibrational modes: (ν) stretching, (δ) in-plane bending, (τ) torsion and (γ) out-of-plane bending.

Non-linear optics analysis. Non-linear optics plays a large role due to potential applications in the future of various processes such as photonic technologies, switching, interconnections, computing, telecommunications, modulation, information processing, signal processing, sensor protection, data storage within information technologies, dynamic image processing, optical industrial, micro- and opto-electronic device designs, since non-linear media can change characteristic features, such as frequency, amplitude, direction, or incident light polarization [38]. In this connection, high interest in low-cost and high-performance non-linear optical (NLO) compounds has become a popular research topic in recent years. The NLO analysis of synthesized novel compounds provides a basis for the subsequent experimental research. The presence of extended conjugated π-bond and delocalized π-electron systems in any chemical compound enhance the NLO properties of the compound.

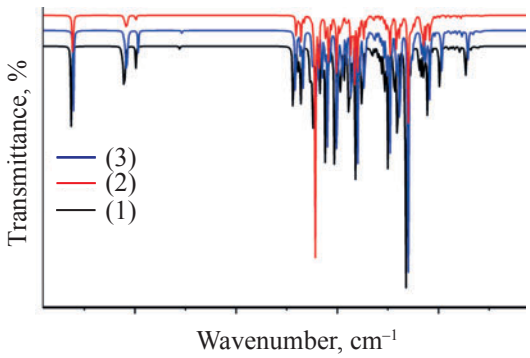

Fig. 2. Experimental and theoretical (1) IR spectra of the thione (2) and thiol (3) forms of **2-SBNS**x

The aforesaid prompted us to perform an NLO analysis of the title compound. For the thione and thiol forms of the compound we calculated, at the B3LYP/6-311++G(d,p) level of theory in the gas phase, the *x*, *y*, and *z* components of the static dipole moment (μ), static polarizability (α) and static first-order hyperpolarizability (β) [39].

The resulting static μ_{total}, α_{total}, Δα, and β_0 values are summarized in Table 7. Judging from these values,

Table 5. Electronic structure parameters for the thiol and thione forms of **2-SBNS**

	Thiol form, Hartree/eV	Thione form, Hartree/eV
LUMO	–0.08111/–2.20706	–0.08914/–2.42556
HOMO	–0.21311/–5.79887	–0.20551/–5.59207
A	0.08111/2.20706	0.08914/2.42556
I	0.21311/5.79887	0.20551/5.59207
ΔE	0.132/3.59181	0.11637/3.16651
χ	0.14711/4.00297	0.147325/4.00882
P_i	–0.14711/–4.00297	–0.147325/–4.00882
ω	0.000714165/0.01943	0.000631443/0.01718
IP	–0.00970926/–0.2642	–0.00857211/–0.23325
S	15.1515/412.283	17.1866/467.658
η	0.066/1.79591	0.058185/1.58325

the thione form has a better the NLO profile than the thiol form. Generally, urea is used as a reference in theoretical NLO studies [40]. The static α_{total}, $\Delta\alpha$, and β_0 parameters calculated for urea at the B3LYP/6-311++G(d,p) level are 5.0480×10^{-24}, 2.0366×10^{-24}, and 7.8782×10^{-31} esu, respectively [38]. Comparing with respective calculated values for **2-SBNS**, we can see that the static α_{total}, $\Delta\alpha$ and β_0 of the latter are about 11.83, 17.35 and 37.43 times (thione form) and 11.35, 15.62 and 20.16 times (thiol form) higher than those of urea. The results suggest that the title compound holds promise for NLO applications.

When viewed energetically, the thione form (–2111.4525 Hartree) has a lower energy than the thiol form (–2111.4265 Hartree). These results may indicate that the molecule prefers the thione form.

Surface and contour maps. The molecular electrostatic potential (MEP) analysis is a reliable method to investigate the chemical reactivity of a

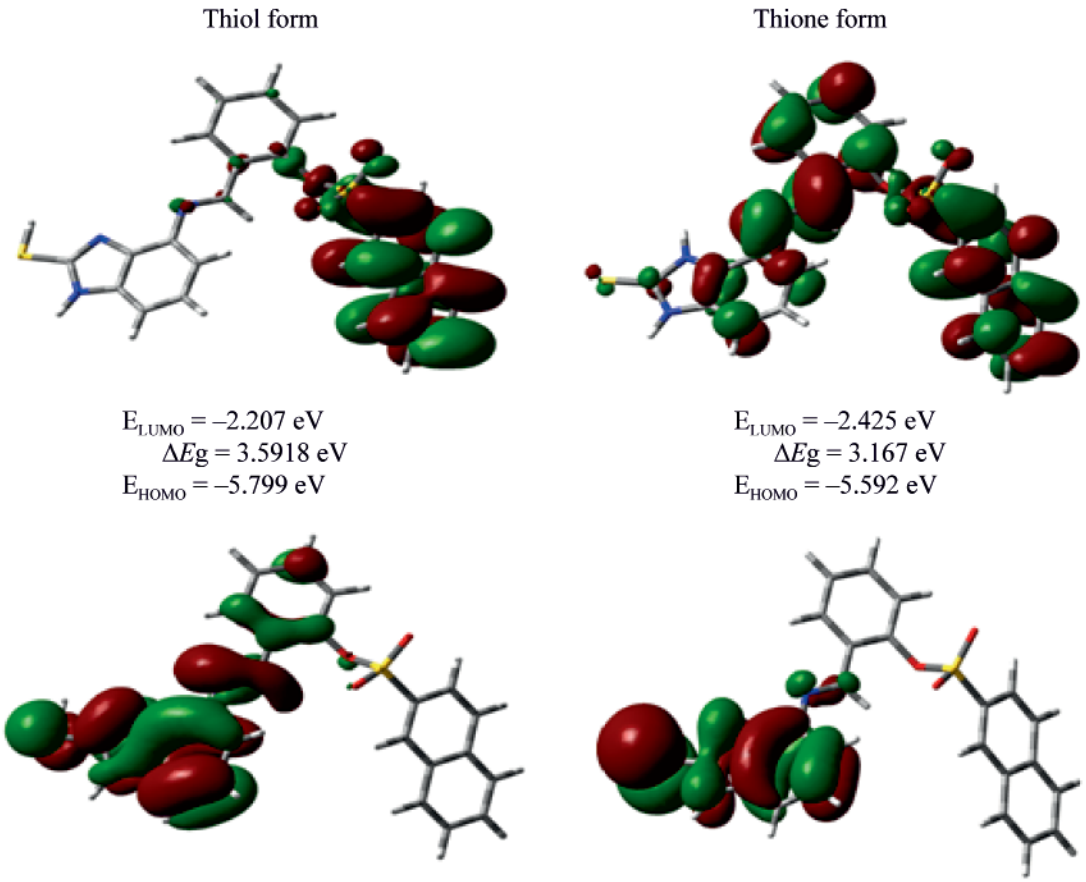

Fig. 3. LUMO and HOMO surfaces for the thiol and thione forms of **2-SBNS**: (burgundy clouds) negative charges and (green clouds) positive charges

Table 6. Calculated thermodynamic parameters of the thiol and thione forms of **2-SBNS**

Rotational temperatures, K	Thiol form	Thione form
A	0.00723	0.00764
B	0.00316	0.00299
C	0.00242	0.00234
Rotational constants, GHz		
A	0.15065	0.15915
B	0.06593	0.06224
C	0.05041	0.04882
Thermal Energies *E*, kcal/mol		
Translational	0.889	0.889
Rotational	0.889	0.889
Vibrational	240.296	242.655
Total	242.073	244.433
Thermal Capacity C_V, cal mol^{-1} K		
Translational	2.981	2.981
Rotational	2.981	2.981
Vibrational	98.668	97.351
Total	104.630	103.312
Entropy *S*, cal mol^{-1} K		
Translational	44.261	44.261
Rotational	37.704	37.739
Vibrational	106.290	103.356
Total	188.256	185.356
Zero-point correction, Hartree/particle	0.358952	0.363315
Thermal correction to energy	0.385769	0.389528
Thermal correction to enthalpy	0.386713	0.390472
Thermal correction to Gibbs free energy	0.297266	0.302404
Sum of electronic and zero-point energies	–2111.067532	–2111.089231
Sum of electronic and thermal energies	–2111.040715	–2111.063017
Sum of electronic and thermal enthalpies	–2111.039771	–2111.062073
Sum of electronic and thermal free energies	–2111.129217	–2111.150142
Zero-point vibration energy, kcal/mol	225.24571	227.98331

Table 7. Total energy, static dipole moment and static polarizability values for **2-SBNS**

Parameters	Thiol form	Thione form
E_{total} , Hartree	–2111.42648381	–2111.45254542
μ_{total} , Debye	2.2610	3.2491
α_{total}, esu	57.2953×10^{-24}	59.7192×10^{-24}
$\Delta\alpha$, esu	31.8211×10^{-24}	35.3435×10^{-24}
β_0 , esu	158.8511×10^{-31}	294.8587×10^{-31}

molecular system, electrophilic and nucleophilic regions. The MEP analysis was carried using B3LYP functional and 6-311++G(d,p) basis set in which the chk file of the optimized structure was used. The MEP surface of the title compound is shown in Fig. 4. The different colors on the MEP surface relate to different electrostatic potentials: the red color represents a negative electrostatic potential, the blue color shows a positive electrostatic potential, and the green color represents a relatively low positive electrostatic potential. The most negative area on the MEP sufrace falls on the N^{42}, N^{43}, N^{44}, O^{45}, O^{46}, O^{47}, S^{48}, S^{49} atoms, implying that these are the most suitable regions for electrophilic attack. On the other hand, the most positive area is localized around the N–H bond of the benzimidazole ring, therefore,

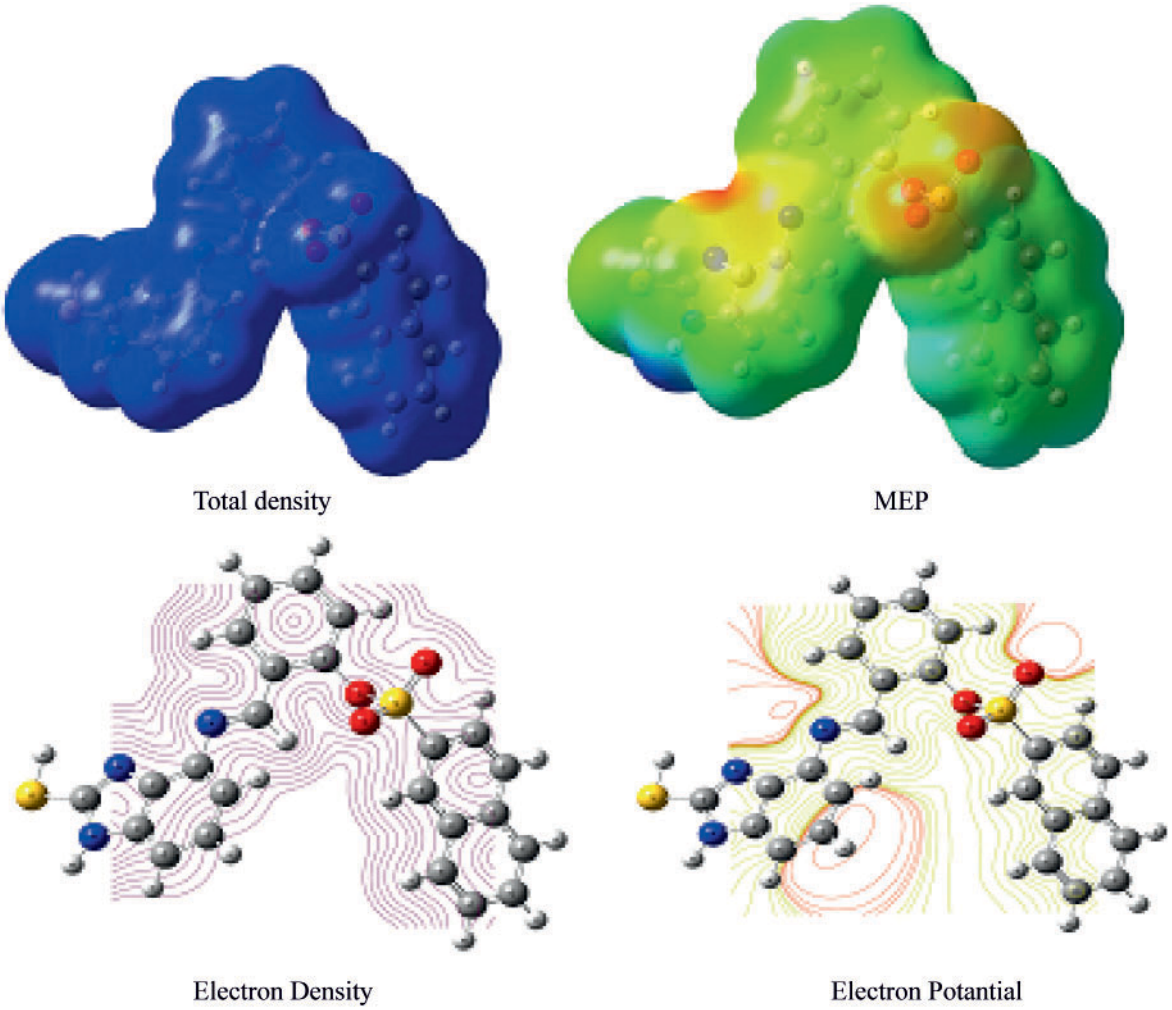

Fig. 4. Calculated molecular surfaces of **2-SBNS**.

this region is the most susceptible to nucleophilic attack.

EXPERIMENTAL

Chemical reagents were purchased from Merck AG, Aldrich, and Fluka. The melting point was determined in open capillary tubes on an Electrothermal melting point apparatus and were uncorrected. The IR spectrum was obtained on a Perkin-Elmer Spectrum One FTIR spectrophotometer. The ^{1}H and ^{13}C NMR spectra were recorded on a Bruker Ultrashield spectrometer at 400 and 100 MHz, respectively, for DMSO-d_6 solutions, internal reference TMS.

Synthesis of 2-[(2-sulfanyl-1*H*-benzo[*d*]imidazol-5-yl)iminomethyl]phenyl naphthalene-2-sulfonate. A solution of 3.12 g (0.01 mol) of 2-[(naphthalene-2-yl)-sulfonyloxy] in 20 mL of acetic acid was treated with 1.65 g (0.01 mol) of 5-amino-2-sulfanylbenzimidazole. The mixture was refluxed for 2 h, cooled to room temperature, and evaporated at 50–55°C in a vacuum. Several recrystallizations of the residue from ethanol gave a pure target product. Yield 4.50 g (98%), yellow crystals, mp 124°C. IR spectrum (KBr), ν, cm^{-1}: 3333 (NH), 1610 (C=N), 1275–1043 (SO_2). ^{1}H NMR spectrum, δ, ppm: 6.73 d ($1H_{arom}$, *J* 8.3 Hz), 6.77 s ($1H_{arom}$), 7.03 d ($1H_{arom}$, *J* 8.4 Hz), 7.25 d ($1H_{arom}$, *J* 8.3 Hz), 7.47 t ($1H_{arom}$, *J* 7.6 Hz), 7.57 t ($1H_{arom}$, *J* 8.1 Hz), 7.62 t ($1H_{arom}$, *J* 8.1 Hz), 7.71 t ($1H_{arom}$, *J* 8.2 Hz), 7.80 d ($1H_{arom}$, *J* 8.7 Hz), 7.96 d ($1H_{arom}$, *J* 8.1 Hz), 8.05 d ($1H_{arom}$, *J* 7.8 Hz), 8.11 d ($2H_{arom}$, *J* 8.6 Hz), 8.32 s ($1H_{arom}$), 8.57 s (1H, N=CH), 12.56 s (1H, NH), 12.59 s (1H, SH). ^{13}C NMR spectrum, δ, ppm: 101.60, 109.86, 116.08, 122.19, 123.61, 127.64, 127.83, 127.90, 127.94, 128.02, 128.07, 129.05, 129.51, 129.94, 130.11, 130.26, 130.82, 131.24, 131.43, 132.63, 132.85, 135.12, 145.68, 148.85, 168.88 (C_{arom}), 152.33 (N=CH).

Quantum-chemical calculations. The molecular geometries (bond angles, bond lengths) were optimized, and the MEP graphs, HOMO and LUMO energies, FMO densities, thermodynamic and electronic properties were calculated, and NLO analysis was performed by the DFT/B3LYP/6-311G++(d,p) method using Gaussian 09W software [30–32]. The ^{1}H and ^{13}C NMR chemical shifts were calculated by the gauge independent atomic orbital (GIAO) approach [33]. The VEDA4 software [34] was used to calculate harmonic vibration frequencies, which were then scaled [35]. The calculated results were obtained immersive via the GaussView 5.0 program [36].

CONCLUSIONS

In this work, a novel 2-[(2-sulfanyl-1*H*-benzo[*d*]-imidazol-5-yl)iminomethyl]phenyl naphthalene-2-sulfonate (**2-SBNS**) was synthesized, and the geometric, spectroscopic, and electronic parameters for the thiol and thione forms of this compound were calculated by the DFT/ B3LYP/6-311G++(d,p) method. The ^{1}H and ^{13}C NMR parameters calculated for the gas phase and DMSO solutions were found to be excellent agreement with the experimental data. Among the calculated IR vibration frequencies, no negative values were found, which showed that the molecule is stable. The vibration frequencies obtained for the thiol and thione forms of the molecule differ from each other and are close to experimental data. Three-dimensional images of the HOMO and LUMO were drawn. The HOMO-LUMO energy gaps for the thiol and thione forms are small and close to each other (3.5918 and 3.1672 eV, respectively). The HOMO and LUMO energies were used to calculate the electronic parameters of **2-SBNS**. The NLO analysis showed that the thiol form of the molecule is more stable than the thione form and is a good non-linear optical compound. Finally, the MEP map was created, where the electrophilic and nucleophilic regions of the molecule are easily identified.

ACKNOWLEDGMENTS

This study was supported by the Kafkas University Scientific Research Projects Coordination (project no. 2014-MMF-43).

CONFLICT OF INTEREST

The authors declare no conflict of interest.

REFERENCES

1. Archie, S.R., Das, B.K., Hossain, M.D.S., Kumar, U., and Shamsur Rouf, A.S., *Int. J. Pharm. Pharm. Sci*., 2017, vol. 9, p. 308. https://doi.org/10.22159/ijpps.2017v9i1.14972
2. Karmaker, N., Noor Lira, D., Kumar Das, B., Kumar, U., and Shamsur Rouf, A.S., *Dhaka Univ. J. Pharm. Sci*., 2017, vol. 16, p. 245. https://doi.org/10.3329/dujps.v16i2.35263
3. Anastassova, N.O., Mavrova, A.T., Yancheva, D.Y., Kondeva-Burdina, M.S., Tzankova, V., Stoyanov, S.S., Shivachev, B.L., and Nikolova, R.P., *Arab. J. Chem*., 2018, vol. 11, p. 353.

https://doi.org/10.1016/j.arabjc.2016.12.003

4. Datar, P.A. and Limaye, S.A., *Anti-Inflammatory Anti-Allergy Agents Med. Chem*., 2015, vol. 14, p. 35. https://doi.org/10.2174/1871523014666150312164625
5. Gaba, M. and Mohan, C., *Med. Chem*., 2015, vol. 5, p. 58. https://doi.org/10.4172/2161-0444.1000243
6. Eswayah, A., Khaliel, S., Saad, S., Sheban, N., Fhid, O., Belaid, A., Alsharif, T., Elforjane, H., Saadalla, Y., and Baga, E., *Am. J. Chem. Appl*., 2017, vol. 4, p. 30.
7. Achar, K.C.S., Hosamani, K.M., and Seetharamareddy, H.R., *Eur. J. Med. Chem*., 2010, vol. 45, p. 2048. https://doi.org/10.1016/j.ejmech.2010.01.029
8. Sethi, P., Bansal, Y., and Bansal, G., *Med. Chem. Res*., 2018, vol. 27, p. 61. https://doi.org/10.1007/s00044-017-2036-1
9. Vasantha, K., Basavarajaswamy, G., Vaishali Rai, M., Boja, P., Pai, V.R., Shruthi, N., and Bhat, M., *Bioorg. Med. Chem. Lett*., 2015, vol. 25, p. 1420. https://doi.org/10.1016/j.bmcl.2015.02.043
10. Shingalapur, R.V., Hosamani, K.M., Keri, R.S., and Hugar, M.H., *Eur. J. Med. Chem*., 2010, vol. 45, p. 1753. https://doi.org/10.1016/j.ejmech.2010.01.007
11. Padalkar, V.S., Borse, B.N., Gupta, V.D., Phatangare, K.R., Umape, P.G., and Sekar, N., *Arab. J. Chem*., 2016, vol. 9, p. S1125. https://doi.org/10.1016/j.arabjc.2011.12.006
12. Lingala, S., Nerella, R., and Sambasiva Rao, K.R.S., *Der Pharma Chem*., 2011, vol. 3, p. 344.
13. Singh Rathee, P., Dhankar, R., Bhardwaj, S., Gupta, M., and Kumar, R., *J. Appl. Pharm*., 2011, vol. 1, p. 127.
14. Soni, B., Ranawat, M.S., Bhandari, A., and Sharma, R., *Int. J. Drug Res. Technol*., 2012, vol. 2, p. 479.
15. Hranjec, M., Pavloviç, G., Marjanoviç, M., Kralj, M., and Karminski-Zamola, G., *Eur. J. Med. Chem*., 2010, vol. 45, p. 2405. https://doi.org/10.1016/j.ejmech.2010.02.022
16. Refaat, H.M., *Eur. J. Med. Chem*., 2010, vol. 45, p. 2949. https://doi.org/10.1016/j.ejmech.2010.03.022
17. Mor, M., Bordi, F., Silva, C., Rivara, S., Zuliani, V., Vacondio, F., Rivara, M., Barocelli, E., Bertoni, S., Ballabeni, V., Magnanini, F., Impicciatore, M., and Plazzi, P.V., *Bioorg. Med. Chem*., 2004, vol. 12, p. 663. https://doi.org/10.1016/j.bmc.2003.11.030
18. Wang, X.J., Xi, M.Y. Fu, J.H., Zhang, F.R., Cheng, G.F., Yin, D.L., and You, Q.D., *Chin. Chem. Lett*., 2012, vol. 23, p. 707. https://doi.org/10.1016/j.cclet.2012.04.020
19. Kumar, J.R., Jawahar, J.L., and Pathak, D.P., *E-J. Chem*., 2006, vol. 3, p. 278. https://doi.org/10.1155/2006/765712
20. Zhu, W. Da, Y., Wu, D., Zheng, H., Zhu, L., Wang, L., Yan, Y., and Chen, Z., *Bioorg. Med. Chem*., 2014, vol. 22, p. 2294. https://doi.org/10.1016/j.bmc.2014.02.008
21. Sharma, M.C., Sharma, S., Sahu, N.K., and Kohli, D.V., *J. Saudi Chem. Soc*., 2013, vol. 17, p. 167. https://doi.org/10.1016/j.jscs.2011.03.005
22. Starcevic, K., Kralj, M., Ester, K., Sabol, I., Grce, M., Pavelic, K., and Karminski-Zamola, G., *Bioorg. Med. Chem*., 2007, vol. 15, p. 4419. https://doi.org/10.1016/j.bmc.2007.04.032
23. Shaker, Y.M., Omar, M.A., Mahmoud, K., Elhallouty, S.M., El-Senousy, W.M., Ali, M.M., Mahmouf, A.E., Abdel-Halim, A.H., Soliman, S.M., and El-Diwani, H.I., *J. Enzyme Inhib. Med. Chem*., 2015, vol. 30, p. 826. https://doi.org/10.3109/14756366.2014.979344
24. Shen, Y.-F., Liu, L., Feng, C.-Z., Hu, Y., Chen, C., Wang, G.-X., and Zhu, B., *Fish Shellfish Immun*., 2018, vol. 81, p. 57. https://doi.org/10.1016/j.fsi.2018.07.005
25. Kerimov, I., Ayhan-Kilcigil, G., Can-Eke, B., Altanlar, N., and Iscan, M., *J. Enzyme Inhib. Med. Chem*., 2007, vol. 22, p. 696. https://doi.org/10.1080/14756360701228558
26. Kenchappa, R., Bodke, Y.D., Telkar, S., and Aruna Sindhe, M., *ACS Chem. Biol*., 2017, vol. 10, p. 11. https://doi.org/10.1007/s12154-016-0160-x
27. Chandrika, N.T. Shrestha, S.K., Ngo, H.X., and Garneau-Tsodikova, S., *Bioorg. Med. Chem*., 2016, vol. 24, p. 3680. https://doi.org/10.1016/j.bmc.2016.06.010
28. Anandarajagopal, K., Tiwari, R.N., Bothara, K., Sunilson, J.A.J., Dineshkumar, C., and Promwichit, P., *Adv. Appl. Sci. Res*., 2010, vol. 1, p. 132.
29. Bayomi, S.M., Maarouf, A.R., Abdel-Aziz, N.I., and Mohamed, A.A.B., *J. Am. Sci*., 2013, vol. 9, p. 42. https://doi.org/10.7537/marsjas091013.06
30. Becke, A.D., *J. Chem. Phys*., 2009, vol. 98, p. 5648. https://doi.org/10.1063/1.464913
31. Lee, C., Yang, W.T., and Parr, R.G., *Phys. Rev. B*, 1988, vol. 37, p. 785. https://doi.org/10.1103/PhysRevB.37.785
32. Frisch, M.J., Trucks, G.W., Schlegel, H.B., Scuseria, G.E., Robb, M.A., Mennucci, B., Petersson, G.A., Nakatsuji, H., Caricato, M., Li, X., Hratchian, H.P., Izmaylov, A.F., Bloino, J., Zheng, G., Sonnenberg, J.L.,

Hada, M., Ehara, M., Toyota, K., Fukuda, R., Hasegawa, J., Ishida, M., Nakajima, T., Honda, Y., Kitao, O., Nakai, H., Vreven, T., Montgomery, J.A., Vreven Jr, T., Peralta, J.E., Ogliaro, F., Bearpark, M., Heyd, J.J., Brothers, E., Kudin, N., Staroverov, V.N., Kobayashi, R., Normand, J., Raghavachari, K., Rendell, A., Burant, J.C., Iyengar, S.S., Tomasi, J., Cossi, M., Rega, N., Millam, J.M., Klene, M., Knox, J.E., Cross, J.B., Bakken, V., Adamo, C., Jaramillo, J., Gomperts, R., Stratmann, R.E., Yazyev, O., Austin, A.J., Cammi, R., Pomelli, C.J., Ochterski, W., Martin, L.R., Morokuma, K., Zakrzewski, V.G., Voth, G.A., Salvador, P., Dannenberg, J.J., Dapprich, S., Daniels, A.D., Farkas, O., Foresman, J.B., Ortiz, J.V., Cioslowski, J., and Fox, D.J., *Gaussian 09*, Revision C.01, Gaussian, Inc., Wallingford, CT. 2009.

33. Wolinski, K. Hinton, J.F., and Pulay, P., *J. Am. Chem. Soc*., 1990, vol. 112, p. 8251. https://doi.org/10.1021/ja00179a005
34. Jamróz, M.H., *Vibration Energy Distribution Analysis*, VEDA 4 program, Warsaw, 2004.
35. Merrick, J.P., Moran, D., and Radom, L., *J. Phys. Chem*., 2007, vol. 111, p. 11683. https://doi.org/10.1021/jp073974n
36. Dennington II, R., Keith, T., and Millam, J., *GaussView*, Semichem, Inc., Shawnee Mission, KS, 2007.
37. Fukui, K., Yonezawa, T., and Shingu, H.J., *J. Chem. Phys*., 1952, vol. 20, p. 722. https://doi.org/10.1063/1.1700523
38. *Nonlinear Optics of Organic Molecules and Polymers*, Nalwa, H.S. and Miyata, S., Eds., Boca Raton: CRC Press, 1997.
39. Öztürk, N., Özdemir, T., Alpaslan, Y.B., Gökce, H., and Alpaslan, G., *Bilge Int. J. Sci. Technol. Res*., 2018, vol. 2, p. 56. https://doi.org/10.30516/bilgesci.354763
40. *Molecular Non linear Optics: Materials, Physics and Devices*, Zyss, J., Ed., Boston: Academic Press, 1994.